Cell Reports
Resource

Interactome of Two Diverse RNA Granules Links mRNA Localization to Translational Repression in Neurons

Renate Fritzsche,[1,5] Daniela Karra,[1,2,5,6] Keiryn L. Bennett,[3] Foong yee Ang,[1,4] Jacki E. Heraud-Farlow,[1,7] Marco Tolino,[1] Michael Doyle,[1] Karl E. Bauer,[1,4] Sabine Thomas,[1,2,4] Melanie Planyavsky,[3] Eric Arn,[1,2] Anetta Bakosova,[1] Kerstin Jungwirth,[1,2] Alexandra Hörmann,[1,8] Zsofia Palfi,[1] Julia Sandholzer,[1,11] Martina Schwarz,[1,9] Paolo Macchi,[1,2,10] Jacques Colinge,[3] Giulio Superti-Furga,[3] and Michael A. Kiebler[1,2,4,*]

[1]Department of Neuronal Cell Biology, Center for Brain Research, Medical University of Vienna, 1090 Vienna, Austria
[2]Max-Planck-Institute for Developmental Biology, 72076 Tübingen, Germany
[3]CeMM Research Center for Molecular Medicine of the Austrian Academy of Sciences, 1090 Vienna, Austria
[4]Department for Anatomy & Cell Biology, Ludwig-Maximilians-University, 80336 Munich, Germany
[5]These authors contributed equally to this work
[6]Present address: Paul-Ehrlich-Institute, 63225 Langen, Germany
[7]Present address: Max F. Perutz Laboratories, University of Vienna, 1030 Vienna, Austria
[8]Present address: Boehringer Ingelheim, 1121 Vienna, Austria
[9]Present address: GMI, 1030 Vienna, Austria
[10]Present address: Centre for Integrative Biology (CIBIO), University of Trento, 38060 Mattarello (TN), Italy
[11]Deceased
*Correspondence: michael.kiebler@med.uni-muenchen.de
http://dx.doi.org/10.1016/j.celrep.2013.11.023

SUMMARY

Transport of RNAs to dendrites occurs in neuronal RNA granules, which allows local synthesis of specific proteins at active synapses on demand, thereby contributing to learning and memory. To gain insight into the machinery controlling dendritic mRNA localization and translation, we established a stringent protocol to biochemically purify RNA granules from rat brain. Here, we identified a specific set of interactors for two RNA-binding proteins that are known components of neuronal RNA granules, Barentsz and Staufen2. First, neuronal RNA granules are much more heterogeneous than previously anticipated, sharing only a third of the identified proteins. Second, dendritically localized mRNAs, e.g., *Arc* and *CaMKIIα*, associate selectively with distinct RNA granules. Third, our work identifies a series of factors with known roles in RNA localization, translational control, and RNA quality control that are likely to keep localized transcripts in a translationally repressed state, often in distinct types of RNPs.

INTRODUCTION

Following transcription, RNA is spliced, modified, and exported into the cytoplasm in ribonucleoprotein particles (RNPs). mRNAs are then either immediately translated by ribosomes or translationally repressed and transported to their final site of function, where they can be locally translated upon demand (Doyle and Kiebler, 2011; Holt and Bullock, 2009; Martin and Ephrussi, 2009; St Johnston, 2005). In the CNS, a subset of mRNAs is transported to dendrites, where they are translated at the synapse. It is widely believed that such local synthesis of new proteins contributes to synaptic plasticity, learning, and memory (Costa-Mattioli et al., 2009; Sutton and Schuman, 2006). However, little is known about the underlying mechanisms.

Several studies have now reported the purification of various RNA granules from different sources (Brendel et al., 2004; Elvira et al., 2006; Jønson et al., 2007; Maher-Laporte et al., 2010; Villacé et al., 2004). To date, these studies yielded a large list of protein interactors with very little overlap between associated proteins. Due to the large variance, our understanding of the molecular composition of neuronal RNA granules (Anderson and Kedersha, 2006; Kiebler and Bassell, 2006) including their functions remains incomplete.

In order to further our knowledge into the molecular mechanism of mRNA localization in the CNS and to investigate a possible link with translational control and mRNA decay, we purified two types of neuronal RNA granules from rat brain using two established markers for neuronal RNA granules: Staufen2 (Stau2) and Barentsz (Btz or CASC3, MLN51). Work from various organisms demonstrated that the best molecular markers to follow RNP transport are Staufen proteins (Köhrmann et al., 1999; Martin et al., 2003; Tang et al., 2001; Zimyanin et al., 2008) and Barentsz (Macchi et al., 2003; Palacios et al., 2004; van Eeden et al., 2001). Using this multistep biochemical approach, we report the protein interactome of both Btz- and

Stau2-RNPs from rat brain: 84 and 65 proteins associate with Btz and Stau2, respectively, with only a third of the proteins being shared between both RNP complexes, e.g., the RNA helicase Upf1, FMRP, and Pur-α among others. Furthermore, the dendritic mRNAs *Arc* and *CaMKIIα* associate preferentially with Btz- and Stau2-RNPs, respectively. These results argue for neuronal RNA granule heterogeneity. Furthermore, Btz- and Stau2-RNPs are distinct from processing bodies or stress granules, representing other types of neuronal RNA granules. In addition, components of the exon junction complex (EJC), eIF4AIII, Y14, and Magoh are only found in Btz- but not in Stau2-RNPs. In contrast, the cap-binding protein CBP80 is found in both Btz- and Stau2-RNPs and colocalizes with Stau2 in neuronal dendrites. Together with the fact that several translational repressors associate with both RNPs, our results suggest that these RNPs are translationally stalled. This experimentally confirms a widely accepted hypothesis that transcripts might be translationally repressed during transport preventing their expression elsewhere (St Johnston, 2005).

Taken together, the Btz and Stau2 interactome suggest that factors involved in RNA localization, translational control, and RNA quality control participate in keeping localized transcripts in a translationally repressed state. This study therefore complements previous work on the RNA level showing that localized transcripts are often found in distinct types of RNPs (Amrute-Nayak and Bullock, 2012; Batish et al., 2012; Mikl et al., 2011; Tübing et al., 2010). It is tempting to speculate that neuronal RNA granules are much more heterogeneous and possibly more dynamic than previously anticipated.

RESULTS

Isolation of Endogenous RNPs

Our goal was to isolate endogenous RNPs from rat brain extracts to decipher the molecular composition of neuronal RNA granules (Kiebler and Bassell, 2006) in order to gain more insight into the underlying mechanism of dendritic mRNA localization. Therefore, we established a multistep biochemical isolation protocol for neuronal RNA granules or RNPs (Figure 1A) based on our previous work (Mallardo et al., 2003). This improved approach comprises three distinct steps: (1) the generation of soluble brain lysates; (2) the enrichment of RNA granules via density gradient centrifugation; and (3) preparative scale immunoprecipitations (IPs) using mono-specific, affinity-purified antibodies that allow the affinity purification of endogenous RNA-protein complexes. In detail, soluble S20 supernatants were generated from E17 rat brain lysates that are depleted for intact cells, cell debris, and large membrane-bound organelles (Mallardo et al., 2003), often yielding high background in IP experiments due to their binding to solid matrices, e.g., protein A Sepharose (data not shown). Next, Optiprep density gradient sedimentation (Kiebler et al., 1999b) was used to enrich for intact RNA-containing Stau2- and Btz-RNPs, while separating them from the main protein peak (Figure 1B) as well as from the endoplasmic reticulum (as shown by the absence of the ER marker calnexin) (Figure 1C). The cofractionation of four known markers for neuronal RNPs, e.g., Btz (Macchi et al., 2003), Stau2 (Goetze et al., 2006; Tang et al., 2001), Stau1 (Kanai et al., 2004; Mallardo et al., 2003), and Poly(A)-binding protein 1 (PABP1) in fractions 4–7 of the Optiprep gradient identified dense RNPs. The presence of PABP1 furthermore suggests that these RNPs are still intact containing 3′-polyadenylated mRNA. Pretreatment of S20 supernatants with RNase shifted a significant portion of the Stau2- and Btz-RNPs toward lighter Optiprep fractions on top of the gradient confirming them as bona fide RNPs (Figure 1D) providing further evidence that the isolated particles are intact and contain RNAs.

We then employed preparative scale IPs using mono-specific, affinity-purified antibodies that recognize two components of neuronal RNA granules: Btz and Stau2 (Kiebler and Bassell, 2006). We have previously generated specific polyclonal antibodies directed against Stau2 (Goetze et al., 2006; Zeitelhofer et al., 2008) and Btz (Macchi et al., 2003; Zeitelhofer et al., 2008) (Figure S1; data not shown) that not only recognize their native antigen(s), but also precipitate endogenous RNPs (Figure 2; data not shown). These antibodies thus allow us to specifically enrich for neuronal RNA granules by affinity purification. Antibodies were chemically crosslinked to the matrix (Sisson and Castor, 1990). Btz and Stau2 preimmune sera (PIS) from the same rabbits served as control. Nonspecific binding to the matrix was blocked by pretreating beads with tRNA and BSA (Harlow and Lane, 1988). Elution of the RNPs from the matrix was performed in a sequential manner: (1) RNA-dependent interactors were eluted by treatment with RNases A and T1 (*RNase Eluate*); and (2) protein-dependent interactors were subsequently eluted by low pH (*Glycine Eluate*). Both eluates were separated by SDS-PAGE and proteins were silver stained (Figures 2A and 2B). Compared to the respective control lanes (PIS-IP for Btz, A, or for Stau2, B), a number of proteins significantly enriched in both IPs indicating that we were able to isolate high molecular weight RNPs.

Systematic Identification of Protein Interactors

Entire gel lanes were excised, 20 regions digested in situ with trypsin, and the samples analyzed by liquid chromatography mass spectrometry (LC-MS). Proteins were identified by searching the MS-generated data against both the mouse and rat International Protein Index protein sequence databases. The rat database was also searched to identify (by homology) unsequenced mouse proteins that were not included in the more complete mouse database. Only proteins that were present in all three independent experiments and identified by at least two peptides (or by three peptides in n-1 experiments) were considered as true positives (Table S1, "Positives"). Importantly, proteins that were also identified in the respective control IPs were excluded from further analysis (Table S2, "Negatives"). In total, 84 proteins were identified in Btz IPs compared to 65 proteins in Stau2 IPs (Figure 2C; Table S1, "Positives"). Only 29 proteins (35% for Btz versus 45% for Stau2) are shared between the two types of RNPs, providing further evidence that both proteins are not simply part of the same RNP and that neuronal RNA granules are much more heterogeneous. This confirms immunofluorescence data showing that Btz and Stau2 do not show significant colocalization in dendritic RNPs in mature neurons (Figure S2), thus implying that RNPs are possibly more dynamic and heterogeneous than previously anticipated.

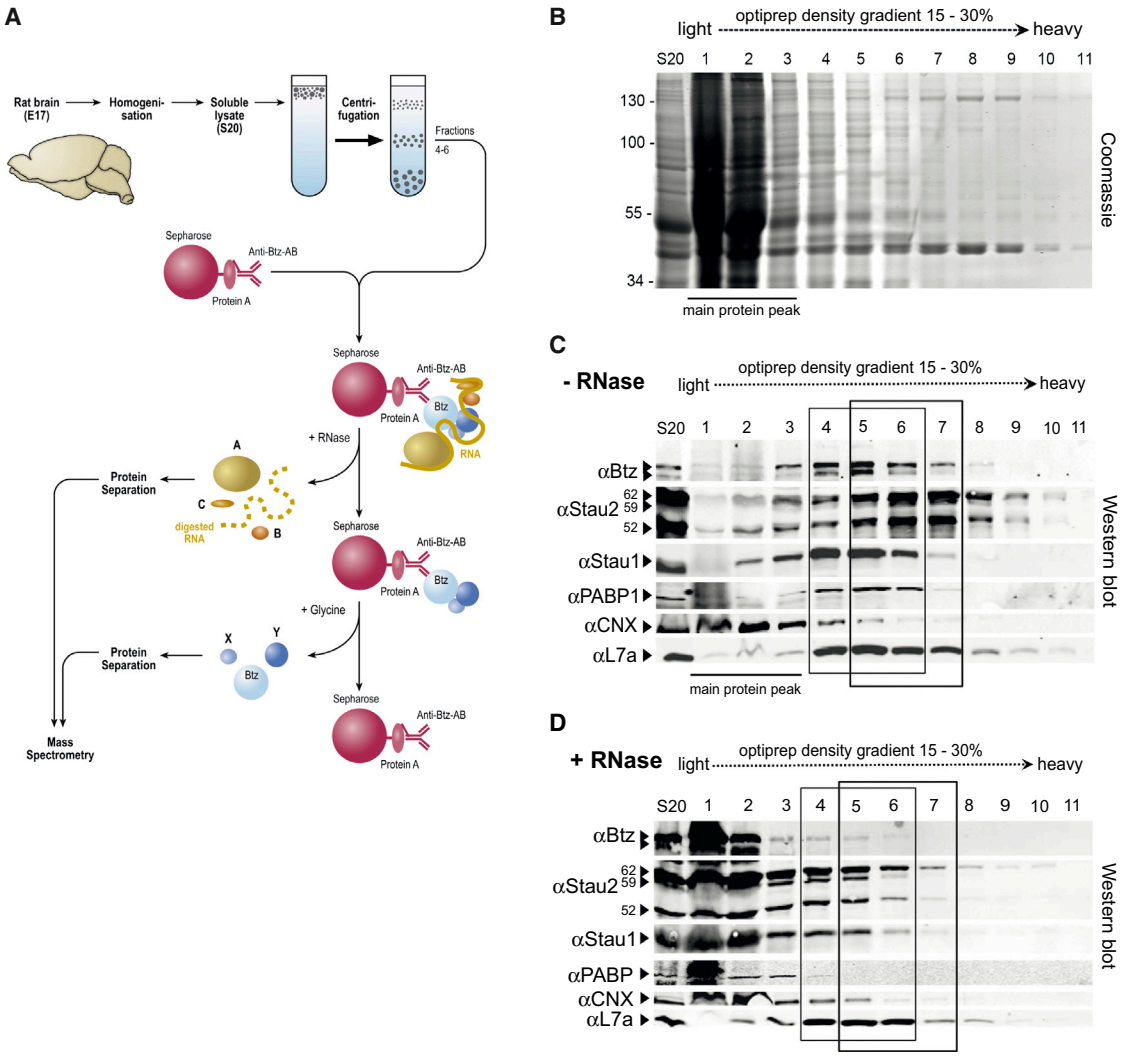

Figure 1. Btz and Stau2 Granules Are RNA-Containing RNPs

(A) Schematic outline of the Btz-RNP purification. The isolation of endogenous Stau2-containing RNPs was essentially the same, except that Stau2 antibodies were used (see also Figure S1).

(B–D) Size fractionation of neuronal RNA granules using Optiprep density gradient centrifugation. 1.5% of each fraction was separated by SDS-PAGE and either stained with Coomassie blue (B) or blotted onto nitrocellulose and probed with the antibodies indicated on the left (C and D). Btz- and Stau2-containing RNPs are enriched in fractions 4–6 (Btz) or fractions 5–7 (Stau2), respectively. Both RNP peaks are clearly separated from free soluble proteins (labeled "main protein peak" in (B) on top of the gradient. The presence of Stau1 as well as the poly(A)-binding protein 1 (PABP1) indicates that the isolated RNPs were still intact. Calnexin (CNX) and ribosomal protein L7a served as markers to follow the fate of ER and ribosomes, respectively. (D) Btz- and Stau2-containing complexes represent true RNA granules. Soluble E17 rat brain lysates were pretreated with RNase A + T1 before loading onto the gradients causing disassembly of RNPs. This shifts all RNP markers, e.g., Btz, Stau2, Stau1, and PABP1, toward lighter fractions on top of the gradient.

See also Figure S1.

To gain insight into the various functions of the identified proteins, we performed gene ontology (GO) term analysis using DAVID (http://david.abcc.ncifcrf.gov). This revealed that five out of the six top categories were related to RNA binding (Figure 2D) as many of the identified proteins are known RBPs: 34/84 for Btz and 31/65 for Stau2: e.g., FMRP, Pur-α, Stau1 (see Table S3 for full list). Among these is a set of RNA helicases that specifically enrich with either Btz- or Stau2-RNPs: Ddx1, eIF4AIII/Ddx48, Mov10. Most significantly, however, many of the identified RBPs have been implicated in RNA localization including translational control or RNP biogenesis: e.g., FMRP, Pur-α, Stau1, and eIF4AIII (Table S3).

Identification of Cargo mRNAs for Btz- and Stau2-RNPs

To further corroborate our findings that neuronal RNA granules are linked to mRNA localization, we investigated whether six established dendritically localized mRNAs are associated with either of the RNPs. Total RNA was isolated from the IP, reverse

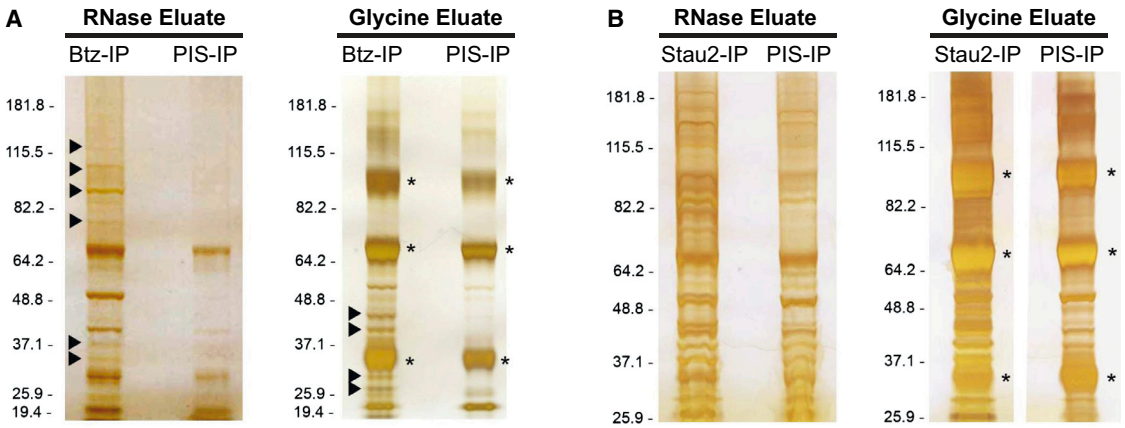

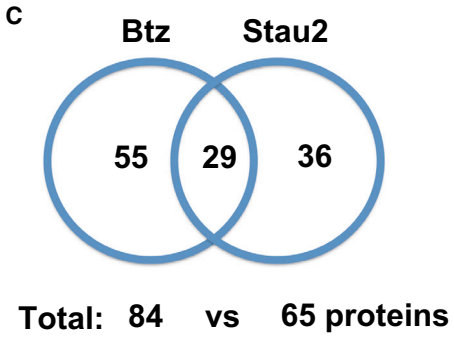

D

		Btz			Staufen 2			
		P-value	Original	Corrected	P-value	Original	Corrected	Shared
1	RNP complex	2.1E-17	22	22	2.3E-21	23	23	12
2	RNA binding	8.0E-19	27	34	6.3E-16	22	31	14
3	Nucleic acid binding	2.8E-11	38	38	2.5E-09	30	30	14
4	RNA localization	1.8E-04	5	12	4.0E-05	5	9	6
5	RNP biogenesis	2.6E-03	5	7	5.9E-02	3	5	1
6	(RNA) Helicase activity	2.3E-03	5	5	8.9E-03	4	4	0
7	Translation initiation factor activity	2.4E-03	3	2	1.8E-02	2	1	1
8	Ribosome	9.1E-04	6	6	2.6E-05	7	7	6
9	Gene silencing by miRNA	n.a.	0	1	4.0E-02	2	2	0

Figure 2. Molecular Composition of Btz- and Stau2-Containing RNPs

(A and B) Preparative IPs from pooled Optiprep gradient fractions (F4-6 for Btz and F5-7 for Stau2, respectively) were performed using Btz (A) or Stau2 (B) antibodies (see also Figures S1 and S2). Control IPs using corresponding preimmune sera (PIS) were performed in parallel. Immunoprecipitates were eluted in two steps (see Figure 1A): first with an RNase A/T1-containing buffer (RNase Eluate) followed by a low pH step (glycine pH 2.5; Glycine Eluate). The resulting eluates were separated by SDS-PAGE and visualized by silver staining. Representative examples are shown. Individual lanes were excised completely and processed for LC-MS (see Table S1 for a complete list of identified interactors and Table S2 for a complete list of proteins that were found in the corresponding PIS-IP lanes). Please note the enrichment of associated proteins in the Btz- (labeled with arrowheads) and Stau2-IP lanes compared to the corresponding PIS-IP lanes. Molecular weight markers are shown on the left. Asterisks mark immunoglobulin G chains that are coeluted by glycine.

(C) Graph indicating the number of proteins identified in Btz- and/or in Stau2-RNPs.

(D) Gene ontology (GO) term analysis of the isolated proteins. Proteins were identified by automated database searching as described in Experimental Procedures against both murine and rat databases, official gene symbols were used to perform GO term analysis using DAVID (http://david.abcc.ncifcrf.gov). For each GO term category, the count (number of proteins identified) and the respective p value are indicated. Proteins with known functions that have been overlooked by GO term were added or false annotations deleted. On the right, the number of shared components between Btz- and Stau2-RNPs are listed (see Table S3 for a complete list).

Original, components identified by DAVID; corrected, missing proteins were added or deleted if falsely annotated; n.a., not applicable. See also Figure S1, Tables S1, S2, and S4.

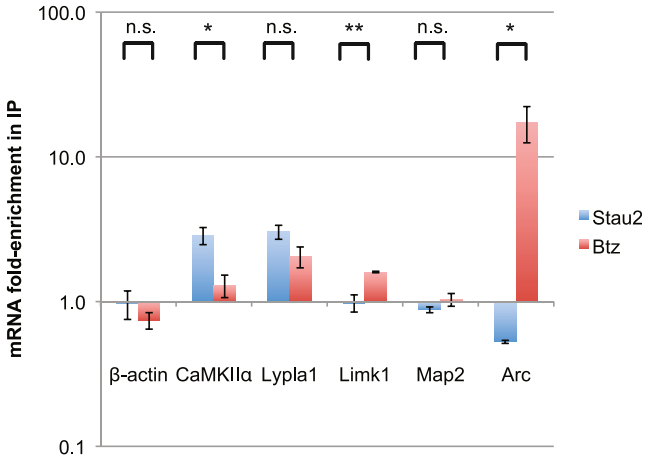

Figure 3. Differential Enrichment of Dendritically Localized mRNAs in Btz- and Stau2-RNPs

Analytical-scale IPs were performed from pooled Optiprep gradient fractions (F5-8 using Stau2 or F4-7 using Btz antibodies). Control IPs using corresponding PIS were performed in parallel. RNA was isolated, and cDNA was synthesized. The enrichment of candidate dendritic mRNAs in the Btz- and Stau2-RNPs was determined by qRT-PCR analysis. Enrichment is calculated as the levels of a given gene in the immunoprecipitated material relative to the IP input, and then normalized for background from the control IP. Error bars represent the SEM from three independent experiments. Students t test was used to calculate statistical significance between Stau2 and Btz. *$p < 0.05$; **$p < 0.01$; n.s., statistically not significant. See also Figure S3 and Tables S3 and S5.

transcribed, and subjected to quantitative RT-PCR (qRT-PCR). The amplified mRNAs were then quantified relative to the input and control IPs for both Btz and Stau2 (Figure 3). The activity-regulated cytoskeletal protein 1 (*Arc*) mRNA and the Lim-domain-containing kinase 1 (*Limk1*) mRNA were specifically enriched in the Btz IP (17.4- and 1.6-fold enrichment, respectively). In contrast, Ca^{2+}/Calmodulin-dependent kinase II alpha (*CaMKIIα*) mRNA was specific to Stau2 (2.9-fold), whereas Lysophospholipase 1 (*Lypla1*) mRNA was found in both RNPs (3.0- and 2.0-fold enrichment in Stau2 and Btz IPs, respectively). These differences in the RNA composition confirm the heterogeneity of the two RNPs previously observed on the protein level. Furthermore, the presence of *Arc* mRNA in Btz-RNPs and *CaMKIIα* mRNA in Stau2-RNPs provides experimental evidence that we have succeeded in enriching for neuronal RNA granules that are involved in RNA localization. Interestingly, eIF4AIII, another component of the EJC (Le Hir and Séraphin, 2008), has been previously linked to dendritic localization and stability of *Arc* mRNA in neurons, providing further validity for its association with Btz-RNPs (Giorgi et al., 2007). In addition to this candidate approach, we recently identified Btz- and Stau2-associated RNAs by microarray and found that only a small set of mRNAs are shared between Btz- and Stau2-RNPs (Heraud-Farlow et al., 2013; data not shown).

The EJC Is Part of Btz-, but Not Stau2-RNPs

From the LC-MS data, we noted that eIF4AIII and Magoh were positive interactors for Btz; however, neither were found with Stau2 (Table S1). For Btz, this was expected as it is a core component of the EJC (Andersen et al., 2006; Bono et al., 2006; Le Hir and Séraphin, 2008) and has been previously linked to mRNA localization (Macchi et al., 2003; van Eeden et al., 2001). The fourth EJC core component, Y14, was detected in Btz-RNPs but was below the threshold to make the cutoff. The EJC assembles on newly formed mRNAs concomitant with splicing and remains associated with that message until it is translated in the cytoplasm. The EJC is important for several stages of mRNA fate, including nuclear export, mRNA stability, localization, and translation (Le Hir and Séraphin, 2008). Furthermore, eIF4AIII has been previously implicated in dendritic localization of *Arc* mRNA in neurons (Giorgi et al., 2007). Therefore, we decided to independently validate whether EJC members were part of our neuronal Btz- and Stau2-RNPs. By western blot, all three core proteins of the EJC were found to be present in Btz- but not in Stau2-IPs (Figure 4A) confirming the LC-MS data.

Additionally, the RNA helicase Upf1 (Regulator of nonsense transcript or Rent), which is not part of the EJC core, but an integral component of the nonsense-mediated mRNA decay (NMD) machinery (Le Hir and Séraphin, 2008), was also identified in both Btz- and Stau2-RNPs. The presence of the EJC and Upf1 indicates that the mRNAs found in Btz-containing RNPs have not yet undergone translation and are translationally repressed. The fact that the EJC is not found in the Stau2-RNPs suggests that the transcripts in these RNPs have already undergone translation, or alternatively, that another mechanism of translational control is active in this case. To further validate this finding, we performed pull-down experiments using brain extracts and GST-Btz or GST-Stau2 as bait. Whereas eIF4AIII bound to GST-Btz, it did not bind to GST-Stau2 (Figure 4B) supporting our previous results. Finally, we performed reverse IPs using eIF4AIII antibodies and soluble S100 extracts and confirmed the interaction between eIF4AIII and Btz (Figure 4C). However, under these conditions, we also detected an interaction between eIF4AIII and Stau2. Interestingly, when we repeated these experiments in the presence of the nonhydrolysable ATP analog, AMP-PNP, to stabilize the binding of the Y14/Magoh heterodimer (Ballut et al., 2005), we could still only detect eIF4AIII, but not Y14/Magoh in Stau2-RNPs (Figure S3). Although further work is necessary, our findings suggest that at least some portion of Stau2 is bound to eIF4AIII, possibly independently of the EJC.

Btz- and Stau2-RNPs Contain the Nuclear Cap-Binding Protein CBP80

A series of studies have reported the presence of general translation factors in neuronal RNPs (Banerjee et al., 2009; Kanai et al., 2004; Krichevsky and Kosik, 2001; Tiedge and Brosius, 1996). Therefore, we looked for translational factors in Btz- and Stau2-RNPs. Three initiation factors in Btz- and two in Stau2-RNPs (Table 1; Figure 2D) were identified by LC-MS. When we validated this by IP and western blot, we did not detect any of the following translation factors in either Btz- or Stau2-RNPs: eEF1A, eIF1A, eIF4G1, eIF3B1, or eIF4E (Figure 5A). This is in line with previous findings for IMP1 (ZBP1) granules (Jønson et al., 2007). Given the absence of eIF4E and the presence of

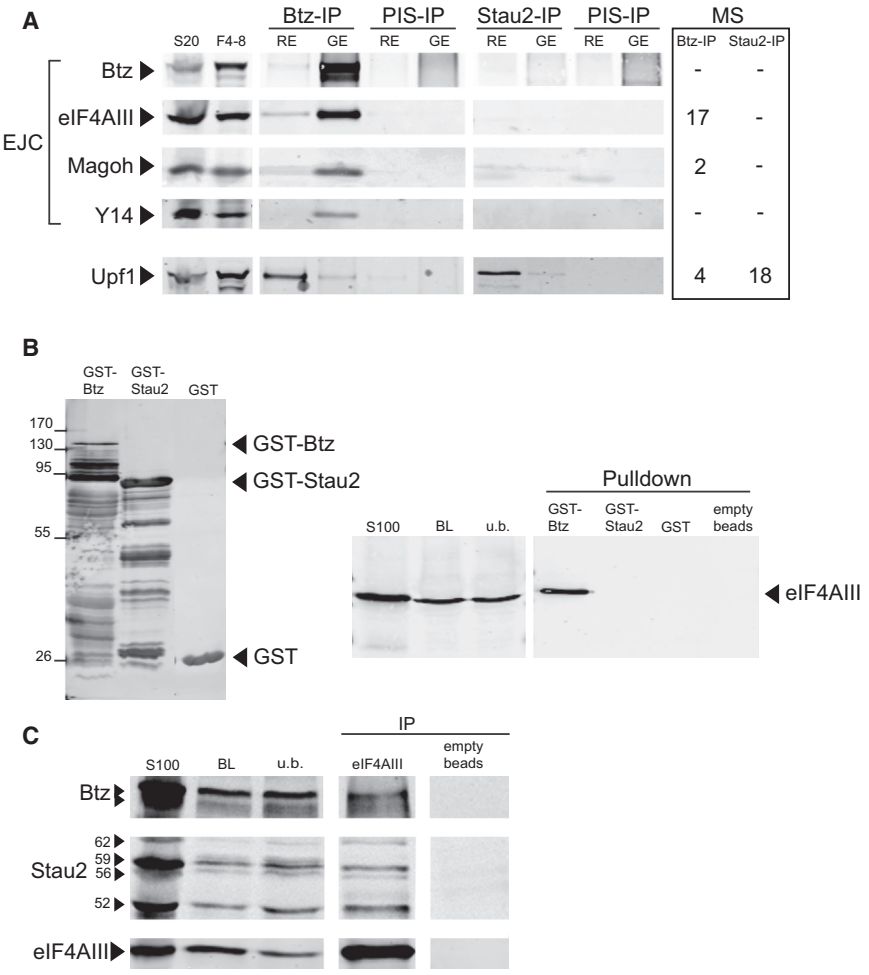

Figure 4. Components of the EJC Are Present in Btz-, but Not in Stau2-RNPs

(A) Analytical-scale IPs were performed from pooled Optiprep gradient fractions (F4–8) using Stau2 or Btz antibodies. Control IPs using corresponding PIS were performed in parallel. Proteins were eluted first with RNase A/T1 (*RNase Eluate* or RE) followed by low pH (glycine pH 2.5; *Glycine Eluate* or GE). Both eluates were separated by SDS-PAGE and analyzed by western blotting with the antibodies indicated on the left. The four EJC core components were detected in the *Glycine Eluates* of Btz IPs, but not in the Stau2 IPs. The EJC-associated RNA helicase Upf1 is present in the *RNase Eluate* of both Btz and the Stau2 IPs. The table on the right summarizes the number of peptide hits found by MS analysis in Btz and/or Stau2 IPs (see Table S1 for a complete interactor list). Peptide hits were added from both *RNase* and *Glycine Eluates*.

(B) GST-pull-down experiments using Btz or Stau2 as bait. Equal amounts of GST-Btz_{FL}, GST-$Stau2^{62}$ and GST protein were separated by SDS-PAGE and analyzed by western blot for GST (left panel). Pull-down experiments were performed from cleared soluble E17 rat brain lysate using GST-Btz and GST-Stau2 chemically crosslinked to glutathione Sepharose beads. Control pull-down experiments using GST-glutathione beads as well as empty beads were performed in parallel. Proteins were eluted with low pH (glycine pH 2.5) and separated by SDS-PAGE. Western analysis shows that eIF4AIII is present in eluates of the Btz-, but not of the Stau2-pull-down.

(C) Analytical scale IPs were performed from cleared soluble lysate using mouse monoclonal eIF4AIII antibodies chemically crosslinked to protein G Sepharose or using empty protein G Sepharose as control. Proteins were eluted with low pH. Both eluates were separated by SDS-PAGE and analyzed by western blotting with antibodies specific for the proteins indicated on the left. Both Btz and Stau2 are detected in eluates of the eIF4AIII-IP (see also Figure S3).

BL, brain lysate; u.b., unbound; empty beads, beads without antibodies. See also Table S4.

the EJC, at least in the Btz-RNPs, we then focused on the nuclear cap-binding protein 80 (CBP80) (di Penta et al., 2009; Hwang et al., 2010). CBP80 is part of the cap-binding complex (CBC), which interacts with Upf1 and plays an important role in NMD and translation. It is thought that the EJC is removed if there are no premature termination codons. Following this, the CBC is replaced by eIF4E and translation can proceed (Kim et al., 2009). Thus, CBP80 and eIF4E are mutually exclusive on a given mRNA. In line with previous findings from other labs (di Penta et al., 2009; Jønson et al., 2007), we found that both (dendritic) Btz- and Stau2-RNPs contain CBP80 (Figure 5A). Likewise, the nuclear PABP, PABPN1, is removed prior to cytoplasmic translation and yet is present in both Stau2- and Btz-RNPs (Table S1). Together, these findings provide another line of evidence that mRNAs present in both neuronal RNPs are translationally repressed.

To visualize the interaction between CBP80 and Stau2 in mature neurons, we performed immunofluorescence microscopy using antibodies directed against either CBP80 or eIF4E (labeled in green) and Stau2 (labeled in magenta). Whereas both CBP80 and eIF4E are expressed in mature hippocampal neurons, only CBP80—but not eIF4E—shows significant colocalization with Stau2 in dendrites (Figures 5B–5D). However, eIF4E is present at synapses of mature hippocampal neurons (Figure 5C; (Vessey et al., 2010). This indicates that the predominantly nuclear CBP80 stays associated with Stau2-RNPs during localization into dendrites of hippocampal neurons. Furthermore, these experiments show that at least some of the identified Stau2 interactors are indeed found in dendritic Stau2-RNPs near synapses.

In addition to general translation factors, ribosomal proteins and even entire ribosomes have been reported to be present in neuronal RNA granules (Elvira et al., 2006; Kanai et al., 2004; Krichevsky and Kosik, 2001). Our systems approach revealed most of the ribosomal proteins as nonspecific interactors, because they were also found in the control IPs using PIS (see Table S2, "Negatives"). However, six ribosomal proteins were specifically associated with Btz- and seven

with Stau2-RNPs (Table S1, "Positives"; Figure 2D). Interestingly, all ribosomal proteins identified are part of the large ribosomal subunit. This is of particular note because stress granules selectively contain components of the small subunit of the ribosome (Anderson and Kedersha, 2008). To further investigate this, we performed western blots following IPs using specific antibodies against the large ribosome subunit protein, L7a, which has been previously reported to directly interact with Stau2 (Duchaîne et al., 2002), as well as antibodies against the small subunit proteins, S3 and S6. Interestingly, all three ribosomal proteins were enriched in both neuronal RNPs (Figure S4). Note, however, that all three ribosomal proteins mentioned above were also present in the PIS IP (Table S2, "Negatives"). Taken together, our data suggest that the isolated RNPs contain translationally repressed mRNAs as CBP80 and PABPN1 are all present but eIF4E, and the vast majority of ribosomal proteins are absent.

A Series of Translational Repressors Associate with Both RNPs

To further investigate the mechanisms of translational control in these neuronal particles, we looked for factors with a known or assumed function in translational regulation. Analysis of the LC-MS data revealed a noticeable enrichment of a series of translational regulators (Table S1, "Positives"; Figures 2D and 6). Some translational regulators preferentially associate with either Btz- or Stau2-RNPs, whereas others are present in both types of RNPs. Many of them, e.g., FMRP, Pur-α, and DDX6, have previously been implicated in RNA localization (Costa-Mattioli et al., 2009).

We therefore performed analytical IPs to validate the presence of the following four RBPs: FMRP, Pur-α, DDX6 (Rck, p54), and RBM14. We also included Pumilio2 (Pum2), because it had been identified as part of dendritic RNPs near synapses (Vessey et al., 2006), although it was not detected by LC-MS. All five RBPs were present in both Btz- and Stau2-RNPs (Figure 6A). Besides these, a substantial number of RBPs were found in the negative interactor list (see Table S2, "Negatives") that had been previously reported as components of neuronal RNA granules: e.g., ZBP1 (IgfII-mRBP1/IMP1), hnRNP-Q (Syncrip), hnRNP-U, YB1, and HuR. They were all enriched in the isolated RNPs, although there were low levels in the control IP as well.

With the exception of HuR that selectively associates with Stau2-RNPs, all four other RBPs were found in both Btz- and Stau2-containing RNPs. Because PABP1 has been reported to localize in cytoplasmic mRNPs containing untranslated mRNAs, its presence in both Btz- and Stau2-containing neuronal RNA granules indicates translational repression. Together, our data support the hypothesis that RNA transport is coupled to translational control (Hüttelmaier et al., 2005).

This prompted us to search for ZBP1 and FMRP, two RBPs with a known role in translational regulation. As described above for eIF4AIII, we performed reverse IPs using soluble S100 fractions and ZBP1 and FMRP antibodies and confirmed the interaction of ZBP1 (Figure 6B) and FMRP (Figure 6C) with Btz and Stau2.

To validate the association of Stau2 and Btz with Pum2, we transfected mature hippocampal neurons with EGFP-Pum2 (in green) and then performed immunostaining using antibodies directed against either Btz or Stau2 (labeled in magenta). Importantly, the pattern of EGFP-Pum2 closely resembles immunostaining of endogenous Pum2 in mature hippocampal neurons (Vessey et al., 2010; Vessey et al., 2006). Interestingly, approximately 27% versus 39% of EGFP-Pum2 colocalizes with both Btz- and Stau2-RNPs in distal dendrites, respectively (Figures 6D–6F). This is consistent with recent findings that Stau2 and Pum2 form a complex that asymmetrically localizes target mRNAs in neural precursor cells (Vessey et al., 2012).

Taken together, these data indicate that a large number of translational repressors are present in both Stau2- and Btz-RNPs keeping them in a translationally stalled state. Furthermore, our data clearly show that Pum2 is found in both dendritic Btz- and Stau2-containing RNPs near synapses thereby suggesting a possible interaction between these RBPs.

RISC Components Are Found in Both Btz- and Stau2-RNPs

In recent years, there has been mounting evidence that miRNAs play critical roles in neurons and at the synapse (Konecna et al., 2009). Interestingly, the LC-MS data from the Stau2- and Btz-RNPs revealed the presence of selective RNA-induced silencing complex (RISC) components in our neuronal RNA granules: e.g., Mov10, Ago2, and PACT (Table S1; Figures 2D and 7A). Indeed, colocalization experiments using EGFP-Mov10 (in green) and antibodies directed against either Btz or Stau2 (in magenta) confirm that approximately 25% versus 45% of Mov10 is present in both Btz- (Figures 7B and 7D) and Stau2-RNPs (Figures 7C and 7D) in distal dendrites, respectively.

In conclusion, our results identified a series of interesting interaction partners for both Btz and Stau2 with possible roles in dendritic mRNA localization, translational control and mRNA decay among others. Furthermore, we present several independent lines of evidence that neuronal RNA granules are much more heterogeneous and possibly dynamic than previously suggested. Finally, our data suggest that both Btz- and Stau2-containing RNPs are translationally repressed.

DISCUSSION

Here, we report the interactome of two distinct neuronal RNA granules isolated from rat brain. The identification of 84 Btz and 65 Stau2 interactors allowed us to systematically compare different types of RNPs and draw important conclusions. First, only one-third of the proteins are shared arguing that neuronal RNA granules are much more heterogeneous than previously anticipated. This is not only true on the protein level, but also on the RNA level (Figure 3; Heraud-Farlow et al., 2013; data not shown). Our biochemical approach allowed us to identify highly conserved members of RNPs by integrating previous proteomes, mostly from cell lines (references in Table S4): e.g., FMRP, the RNA helicase Upf1, the cap-binding protein CBP80, Pur-α, and Mov10. This includes RNA helicases (Jankowsky, 2011) that have previously been implicated with dendritic mRNA transport (Ashraf et al., 2006; Elvira et al., 2006; Giorgi et al., 2007; Kanai et al., 2004). Second, neuronal RNA granules

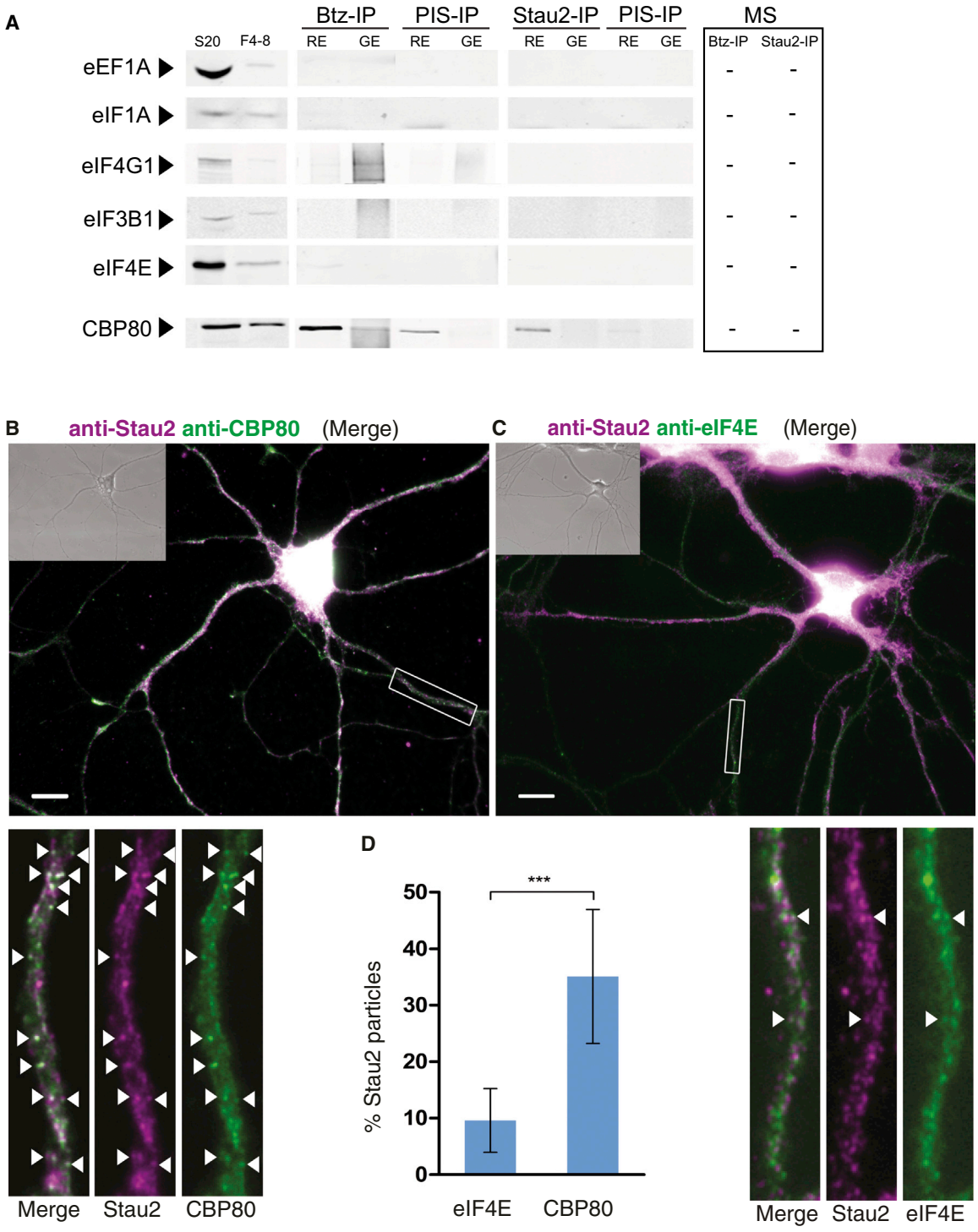

Figure 5. Translational Factors Are Absent, whereas CBP80 Is Present in Both Btz- and Stau2-RNPs

Analytical-scale IPs using Btz or Stau2 antibodies were performed as described in Figure 4.

(A) Known translation factors are absent in both Stau2 and Btz IPs. The nuclear cap-binding protein 80 (CBP80), however, is present in both Stau2 and Btz IPs suggesting that the RNAs in both Btz- and Stau2-RNPs are translationally stalled. The table on the right summarizes the number of peptide hits by MS analysis in Btz and/or Stau2 IPs (see Table S1 for a complete list). Note that ribosomal proteins are mostly absent (see Figure S4).

(B and D) CBP80 is present in dendritic Stau2-RNPs. Eight days in vitro (DIV) dissociated hippocampal neurons were immunostained with mouse anti-Stau2 (in magenta) and rabbit anti-CBP80 (in green).

(legend continued on next page)

only share very few, selected components with P-bodies and stress granules (Anderson and Kedersha, 2006; Zeitelhofer et al., 2008). This confirms a previous hypothesis postulating the existence of various distinct types of neuronal RNA granules (Anderson and Kedersha, 2006). However, it is very likely that individual components might be shared among them or that dynamic remodeling of certain neuronal RNA granules might occur. Third, our data provide experimental support for the previously formulated hypothesis that mRNA localization and translational control are tightly linked (Hüttelmaier et al., 2005). Interestingly, eIF4AIII, a component of the EJC, regulates expression of *Arc* mRNA at the synapse (Giorgi et al., 2007), supporting our findings that EJC members associate with Btz-, but not with endogenous Stau2-RNPs isolated from rat brain. The presence of the EJC in Btz-RNPs—but not in Stau2-RNPs—also suggests that the bound targets have not yet undergone translation. Because *Arc* mRNA has one conserved intron in its 3′ UTR (Giorgi et al., 2007), it is tempting to speculate that Btz and the other EJC components assemble at the intron-exon boundary thereby exerting regulatory functions in addition to its role in NMD, e.g., regulating protein expression or possibly dendritic mRNA localization. A recent study proposes that Btz—by interacting with eIF3—activates translation in fast growing cell lines (Chazal et al., 2013). Fourth, the presence of CBP80 in both (dendritic) Btz- and Stau2-RNPs argues that the bound RNAs are translationally stalled. Such regulation of translation has also been found for other types of RNPs (Chiu et al., 2006; di Penta et al., 2009; Jønson et al., 2007).

Finally, we identify a series of interactors that are known translational regulators, e.g., Pum2, Mov10, and FMRP among others. A genetic screen for memory mutants in *Drosophila* had identified Stau and Pum (Dubnau et al., 2003). It is therefore tempting to speculate that both RBPs exert important functions in dendritic RNPs as previously suggested (Vessey et al., 2010, 2012). Mov10 is an RNA helicase that is part of the RNA-induced silencing complex (Meister et al., 2005) and that is involved in repressing *CaMKII*α mRNA at the synapse (Banerjee et al., 2009).

In conclusion, this work identifies the molecular machinery underlying two types of neuronal RNPs. Furthermore, we provide insights into RNA localization in neurons as our data argue strongly for neuronal RNA granule heterogeneity. Finally, we identify a series of translational regulators that are likely to keep transcripts translationally stalled during transport to their final location in neurons.

EXPERIMENTAL PROCEDURES

Reagents Used in This Study

All antibodies, constructs, antigens, and GST-tagged proteins (for pull-down experiments) used in this study are described in the Supplemental Experimental Procedures.

Preparation of Rat Brain Homogenate

Forty-five brains from 17-day-old rat embryos (E17) were homogenized on ice in 5 ml extraction buffer (EB, 25 mM HEPES [pH 7.3], 150 mM KCl, 8% glycerol, 0.1% NP-40, 1 mM DTT, protease inhibitor cocktail [Roche], 40 U/ml RNase inhibitors [Ribolock, Fermentas]), using a motor-driven dounce homogenizer applying two strokes at 200 rpm and 12 strokes at 1,000 rpm. Brain lysates were centrifuged at 20,000 × *g* for 15 min at 4°C to separate cell debris and nuclei from the soluble S20 supernatant. Similar results were obtained using brains from young adult rats (data not shown).

For GST pull-downs or for FMRP-, ZBP1- and eIF4AIII-IPs, brain lysate was used after high-speed centrifugation. In brief, the soluble lysate was centrifuged two times at 20,000 × *g* for 5 min at 4°C and one time at 100,000 × *g* for 30 min at 4°C to yield an S100 brain lysate. For IPs and pull-downs, proteins were diluted with 1 × EB to a final concentration of 14 mg/ml.

Optiprep Density Gradient Centrifugation

Soluble supernatant (1.7 ml) of homogenized brain lysate (S20) was layered on top of a 10 ml 15%–30% linear Optiprep (Axis Shield) density gradient and centrifuged in a swinging bucket rotor (SW41, Beckman Coulter Genomics) at 280,000 × *g* at 4°C for 2.5 hr. Eleven 900 µl fractions were collected from the top to the bottom of the gradient, frozen in liquid nitrogen, and stored at −80°C. Samples of 10 µl of each fraction were boiled in SDS protein gel sample buffer and subjected to western blotting. To disrupt RNPs, lysates were treated with 100 µg RNase A/T1 mix for 30 min at room temperature (RT) prior to Optiprep density gradient centrifugation.

Immunoprecipitations

For preparative IPs, 300 µg of affinity-purified Btz and Stau2 antibodies or equivalent amounts of corresponding preimmune sera (PIS) were chemically crosslinked to 300 µg protein A Sepharose (PAS) beads (GE Healthcare/Amersham). Antibody-bound Sepharose beads were equilibrated with 0.2 M triethanolamine (pH 9.5) (TEA buffer), and crosslinking was done using 40 mM dimethyl-pimelimidate (DMP) in 200 mM triethanolamine (pH 9.5) (3 × 45 min at RT). After each crosslinking step, beads were washed for 2 × 10 min in 200 mM ethanolamine (pH 8) at RT. The same amount of PAS beads without antibodies served as additional negative control (data not shown). Antibody-bound PAS beads were blocked with 300 µg of yeast tRNAs (Roche) and 1.5 mg BSA (Fermentas) in 1 × EB for 60 min rotating at 4°C. Pooled RNP-containing gradient fractions (F4-6 for Btz, F5-7 for Stau2) were precleared with PAS for 1 hr and allowed to bind to antibody-coupled beads for 90 min at 4°C. Beads were washed four times with 1 × EB and two times with PBS containing 1 mM $MgCl_2$. Proteins were eluted with 600 µl of elution buffer containing RNases (200 µg/ml RNase A/T1 [Fermentas] in PBS [pH 7.1]) for 54 min at RT. After additional washing steps in EB and H_2O, the remaining bound proteins were eluted using a low pH buffer (0.2 M glycine pH 2.5) for 10 min rotating at RT and immediately neutralized in 1 M Tris-HCl (pH 8.5). Proteins eluted with either RNases or glycine were processed for LC-MS. Samples were alkylated with iodoacetamide and separated on a 4%–12% bis-Tris gel (NuPAGE, Invitrogen). After visualization of the proteins by silver staining, entire lanes were sliced into 20 pieces and digested in situ with modified porcine trypsin (Promega) essentially as described (Shevchenko et al., 1996). Prior to analysis by nanoLC-MSMS, tryptically digested samples were purified and concentrated via customized reversed-phase columns adapted from Rappsilber et al. (2003).

Analytical IPs were performed as described above, except that 100 µg of antibodies or equivalent amounts of the corresponding PIS were crosslinked to 50 µg of PAS. S20, S100 brain lysates, or pooled gradient fractions (F4-8) were used as indicated and 2 mM AMP-PNP was added before the IP where indicated (Figure S3). Proteins eluted with RNases or glycine were precipitated

(C and D) In contrast, eIF4E that competes with CBP80 for cap binding shows very little colocalization with Stau2 in dendritic RNPs. Seven DIV neurons were immunostained with rabbit Stau2 (in magenta) and mouse eIF4E antibodies (in green). Boxes represent magnification of depicted areas. Arrowheads mark colocalization events. Scale bar: 10 µm. (D) Graph showing the percentage of Stau2 particles colocalizing with CBP80 or with eIF4E in dendrites (n = 18,20 or n = 33,31, respectively). ***Statistically significant ($p < 0.001$).
See also Figure S4 and Table S4.

Cell PRESS
Open ACCESS

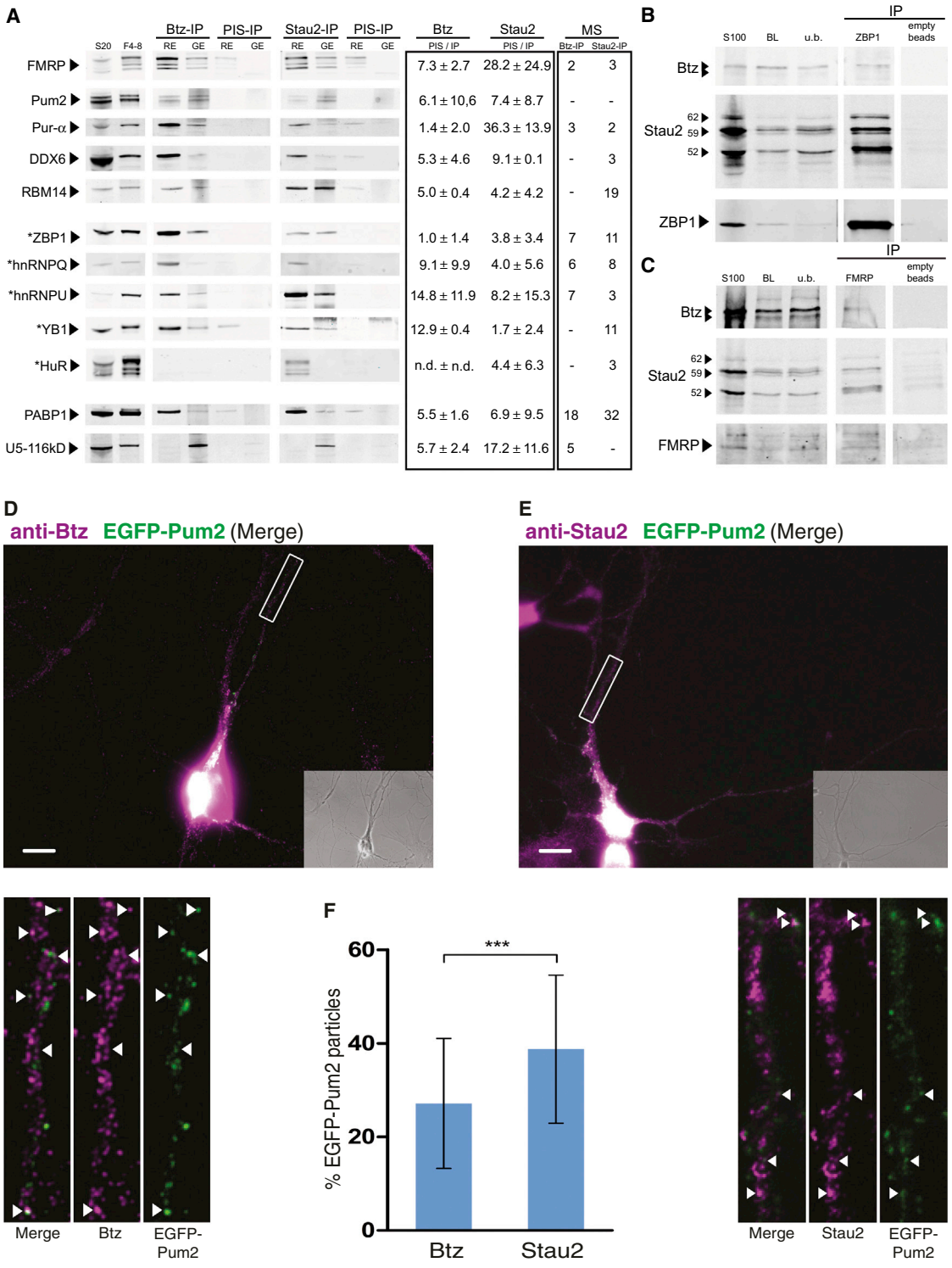

Figure 6. A Series of Translational Repressors Enrich in Both Btz- and Stau2-RNPs

(A) Analytical-scale IPs using Btz or Stau2 antibodies were performed as described in Figure 4. (A) shows the presence of translational repressors FMRP, Pum2, Pur-α, DDX6, RBM14, ZBP1, hnRNP Q (Syncrip), hnRNP U, and YB1 in both Btz and Stau2 precipitates, whereas HuR is only in the Stau2 eluate. The presence of PABP1 in both eluates indicates the presence of mRNA in both Btz- and Stau2-RNPs and the intactness of the RNA granules. In the box in the middle of the panel, protein levels in the Btz and Stau2 IPs were quantified in comparison to their corresponding PIS IP. Band intensities were measured with ImageJ. The values represent the percentage of the PIS to the signal and are the mean ± SD of three to five experiments (PIS/IP, see Experimental Procedures for details). With the

(legend continued on next page)

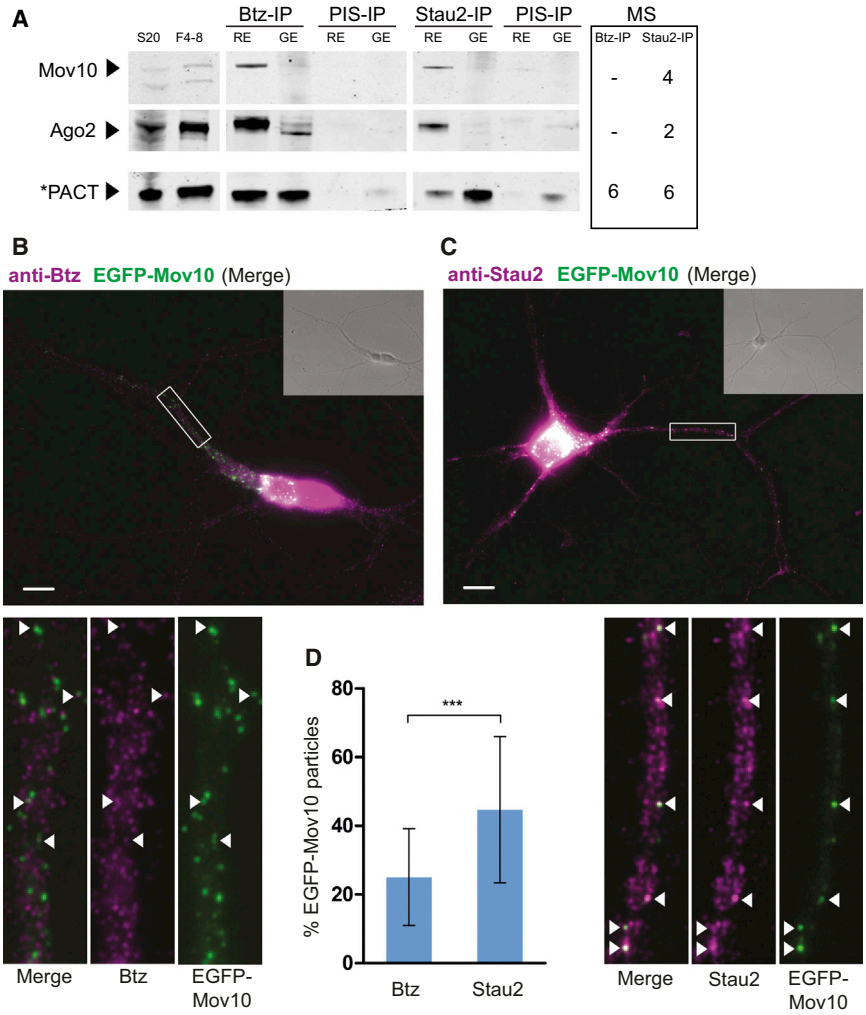

Figure 7. Selected RISC Proteins Are Found in Both Dendritic Btz- and Stau2-RNPs

(A) Components of the RNA-induced silencing complex (RISC), Mov10, Ago2, and PACT are present in both Btz- and Stau2-RNPs. Analytical IPs using Btz or Stau2 antibodies were performed as described in Figure 4. PACT was originally identified in the corresponding PIS-IPs (see negative interactor list, Table S2).

(B–D) Mov10 shows significant colocalization with both Btz (B) and Stau2 (C) in dendritic RNPs. Nine DIV (B) or 11 DIV (C) dissociated hippocampal neurons were transfected with EGFP-Mov10 (in green) and immunostained with either rabbit Btz (B) or rabbit Stau2 (C) (both in magenta) antibodies. Boxes represent magnification of depicted areas. Arrowheads mark colocalization events. Scale bar: 10 μm. (D) Graph showing the percentage of EGFP-Mov10 particles colocalizing with Btz or Stau2 in dendrites (n = 46 or n = 54, respectively). ***Statistically significant ($p < 0.001$). See also Table S4.

as described (Wessel and Flügge, 1984) and analyzed by western blotting. Protein levels were quantified using ImageJ. Values shown in Figure 6A represent the percentage of background (PIS) to signal (IP) and are the mean ± SD of three to five experiments. Please note that, in some cases, background levels could not be determined, therefore preventing us from expressing values as IP/PIS.

For IP of RNAs and qRT-PCR, 100 μg of affinity-purified Btz or Stau2 antibodies and equal amounts of the corresponding PIS were individually coupled to 50 μl of PAS beads (Sigma) and blocked as above. Pooled RNP-containing gradient fractions were precleared with PAS, and 50 μl of the precleared gradient fractions was removed for RNA extraction to serve as input control. The remaining precleared fractions were divided equally among the coupled beads and allowed to bind for 90 min rotating at 4°C. Beads were washed 2 × EB (with 0.5% NP40), 2 × EB (with 0.1% NP40), and 2 × 5 mM Tris (pH 7.4), 100 mM NaCl. Total RNA was isolated directly from the beads and from the input control using a mirVana miRNA Isolation Kit (Ambion). 0.5 μg of input RNA, 0.5 μg of IP RNA, and an equal volume of PIS RNA was taken as templates for random hexamer primed cDNA synthesis using SuperScript III reverse transcriptase (Invitrogen) in a 20 μl reaction volume. cDNAs were diluted 1:10, and 3 μl was used to perform qRT-PCR in a 25 μl final volume using IQ SYBR Green Supermix (Bio-Rad) and gene-specific primers (Table S5) on a MyiQ iCycler (Bio-Rad) according to the manufacturer's instructions. Quantification of gene expression was calculated according to the ΔΔCt method using the average of two independent reference genes. Experiments were repeated with RNA isolated from three independent IPs. Statistical significance using a Student's t test was considered significant if $p < 0.05$.

Liquid Chromatography Mass Spectrometry and Data analysis

Three independent IP experiments for Stau2 were analyzed and two independent IP experiments for Btz. Samples were analyzed by data-dependent nanocapillary reversed-phase LC-MSMS using customized 75 μm inner diameter columns packed with C18 3 μm diameter Reprosil beads (Maisch) on a nanoLC system (Agilent Technologies) coupled to a quadrupole time-of-flight

exception of U5-116 kDa and ZBP1 (both were not detectable in the control lanes), levels of the *RNase Eluate* were quantified. The table on the right summarizes the number of peptides found by MS analysis in Btz and/or the Stau2 IPs (see Table S1 for a complete list). Peptide hits were added together from both *RNase* and *Glycine Eluates*. Proteins labeled by an asterisk were originally identified in the corresponding PIS-IPs (see negative interactor list, Table S2).

(B and C) The translational regulatory factors, ZBP1 and FMRP, are enriched in both Btz- and Stau2-RNPs. Analytical IPs using mouse monoclonal ZBP1 (B) or mouse monoclonal FMRP (C) antibodies were performed as in Figure 4 and analyzed by western blotting. Both Btz and Stau2 are detected in the eluates of both the ZBP1- and the FMRP-IP.

(D–F) Pum2 shows significant colocalization with both Btz and Stau2 in dendritic RNPs. Fourteen DIV (D) and 8 DIV (E) dissociated hippocampal neurons were transfected with EGFP-Pum2 (in green) and immunostained with either rabbit Btz (D) or rabbit Stau2 (E) (both in magenta) antibodies. Boxes represent magnification of depicted areas; arrowheads mark colocalization events. Scale bar: 10 μm. (F) Graph showing the percentage of EGFP-Pum2 particles colocalizing with Btz or with Stau2 in dendrites (n = 51 or n = 47, respectively). ***Statistically significant ($p < 0.001$).

See also Table S4.

(QTOF) mass spectrometer (QTOF Premier or QTOF Ultima, Waters). Data-dependent acquisition was performed for 60 min using one MS channel for every three MSMS channels and a dynamic exclusion for selected ions of 60 s.

Proteins were identified by automated database searching (Mascot, Matrix Science) against the rat and mouse International Protein Index protein sequence databases (IPI, versions 3.21 and 3.26, European Bioinformatics Institute, http://www.ebi.ac.uk/IPI). This compilation of entries from Swiss-Prot, TrEMBL, RefSeq, and Ensembl was appended with human keratin proteins. Search parameters were as follows: MS and MSMS tolerances of 20 or 15 ppm and 0.1 or 0.05 Da, respectively, tryptic specificity allowing for 1 missed cleavage site, fixed modification of carbamidomethylation of cysteine residues, and variable modification of oxidation of methionine residues. Criterion for a positive protein identification was identification of a minimum of two peptides of length of six or more amino acids with a Mascot peptide score of $\geq$20. A false-positive detection rate of <1% was estimated by searching a reversed database. Protein grouping on the basis of shared peptides was realized by an in-house Perl script.

Gene ontology (GO) term analysis was performed using DAVID (http://david.abcc.ncifcrf.gov). To be able to search for rat and mouse proteins at the same time, the official gene symbols ("gene name") were selected for the identified proteins from the UniProtKB/Swiss-Prot database (http://www.ebi.ac.uk/swissprot). In DAVID, the following functional categories were analyzed for both Btz and Stau2: biological pathway (BP), cellular compartment (CC), molecular function (MF), as well as interpro and kegg to identify protein domains. In Figure 2D, proteins with known functions that have been overlooked by GO term were added or false annotations deleted ("corrected").

GST-Pull-Downs

Thirty micrograms of GST-Btz_{FL}, GST-$Stau2_{FL}$ or GST proteins was bound and crosslinked to 30 µl of glutathione Sepharose following the same protocol as for crosslinking antibodies to PAS. Brain lysate was centrifuged at high speed as described above and diluted in 1 × EB to obtain a protein concentration of approximately 14 µg/µl. Brain lysates were precleared with glutathione Sepharose beads by rotating them 1 hr at 4°C. Precleared brain lysate was incubated with the beads for 90 min rotating at 4°C. Approximately 1 ml of brain lysate was used for each pull-down experiment. Beads were washed four times with 1 × EB and two times with ddH_2O, and proteins were eluted in 120 µl low pH buffer (0.2 M glycine pH 2.5) for 10 min rotating at RT and neutralized in 30 µl 1 M Tris-Cl (pH 8.5). Eluted proteins were precipitated using chloroform/methanol as described above and analyzed by western blotting.

Hippocampal Cultures, Transient Transfections, and Immunostainings

Rat hippocampal neurons were cultured, transiently transfected, and immunostained as described (Goetze et al., 2006). Figure legends indicate the respective age of neurons in culture. For quantifying colocalizing events, a set of images—either double immunofluorescence stainings or immunostainings of hippocampal neurons that were transfected with GFP-tagged Pum2 or Mov10—were selected and manually scored by at least two independent observers in a blind manner. Colocalizing events of either Btz or Stau2 with EGFP-Pum2 or EGFP-Mov10 were confirmed by linescan (MetaMorph 6.3, Universal Imaging). Statistical analysis was performed using Prism (GraphPad) and considered significant if $p < 0.05$.

SUPPLEMENTAL INFORMATION

Supplemental Information includes Supplemental Experimental Procedures, four figures, and five tables and can be found with this article online at http://dx.doi.org/10.1016/j.celrep.2013.11.023.

ACKNOWLEDGMENTS

This manuscript is dedicated to Julia Sandholzer for her excellent scientific contributions. We thank Franziska Busch, Inge Kepert, Ingrid Kieweg, Bastian Popper, and Sabine Spath for assistance, Drs. Egon Ogris and Stefan Schuechner for raising mouse monoclonal Stau2 antibodies, and Drs. Paul Anderson, Dorothee Dormann, Stefan Hüttelmaier, Eckhard Jankowsky, Gunter Meister, and Jernej Ule for discussions. This work was supported by the Schram-Foundation (T287/14958/2005), the ESF/Eurocores program RNA Quality (FWF I127-B12), an FWF grant (FWF P20583-B12), the SFB RNA-Seq (FWF F4314-B09), the Doktoratskolleg RNA Biology (FWF W1207-B09), a project grant from the HFSP (RGP24/2008), the Herzfelder foundation (Vienna, Austria), and the Max-Planck Society (all to M.A.K.), a FWF grant (P19514-B09 to P.M.), and a DOCforte PhD fellowship from the Austrian Academy of Sciences to Renate Fritzsche.

Received: June 7, 2013
Revised: October 7, 2013
Accepted: November 12, 2013
Published: December 19, 2013

REFERENCES

Amrute-Nayak, M., and Bullock, S.L. (2012). Single-molecule assays reveal that RNA localization signals regulate dynein-dynactin copy number on individual transcript cargoes. Nat. Cell Biol. *14*, 416–423.

Anderson, P., and Kedersha, N. (2006). RNA granules. J. Cell Biol. *172*, 803–808.

Anderson, P., and Kedersha, N. (2008). Stress granules: the Tao of RNA triage. Trends Biochem. Sci. *33*, 141–150.

Andersen, C.B., Ballut, L., Johansen, J.S., Chamieh, H., Nielsen, K.H., Oliveira, C.L., Pedersen, J.S., Séraphin, B., Le Hir, H., and Andersen, G.R. (2006). Structure of the exon junction core complex with a trapped DEAD-box ATPase bound to RNA. Science *313*, 1968–1972.

Ashraf, S.I., McLoon, A.L., Sclarsic, S.M., and Kunes, S. (2006). Synaptic protein synthesis associated with memory is regulated by the RISC pathway in Drosophila. Cell *124*, 191–205.

Ballut, L., Marchadier, B., Baguet, A., Tomasetto, C., Séraphin, B., and Le Hir, H. (2005). The exon junction core complex is locked onto RNA by inhibition of eIF4AIII ATPase activity. Nat. Struct. Mol. Biol. *12*, 861–869.

Banerjee, S., Neveu, P., and Kosik, K.S. (2009). A coordinated local translational control point at the synapse involving relief from silencing and MOV10 degradation. Neuron *64*, 871–884.

Batish, M., van den Bogaard, P., Kramer, F.R., and Tyagi, S. (2012). Neuronal mRNAs travel singly into dendrites. Proc. Natl. Acad. Sci. USA *109*, 4645–4650.

Bono, F., Ebert, J., Lorentzen, E., and Conti, E. (2006). The crystal structure of the exon junction complex reveals how it maintains a stable grip on mRNA. Cell *126*, 713–725.

Brendel, C., Rehbein, M., Kreienkamp, H.J., Buck, F., Richter, D., and Kindler, S. (2004). Characterization of Staufen 1 ribonucleoprotein complexes. Biochem. J. *384*, 239–246.

Chazal, P.E., Daguenet, E., Wendling, C., Ulryck, N., Tomasetto, C., Sargueil, B., and Le Hir, H. (2013). EJC core component MLN51 interacts with eIF3 and activates translation. Proc. Natl. Acad. Sci. USA *110*, 5903–5908.

Chiu, Y.L., Witkowska, H.E., Hall, S.C., Santiago, M., Soros, V.B., Esnault, C., Heidmann, T., and Greene, W.C. (2006). High-molecular-mass APOBEC3G complexes restrict Alu retrotransposition. Proc. Natl. Acad. Sci. USA *103*, 15588–15593.

Costa-Mattioli, M., Sossin, W.S., Klann, E., and Sonenberg, N. (2009). Translational control of long-lasting synaptic plasticity and memory. Neuron *61*, 10–26.

di Penta, A., Mercaldo, V., Florenzano, F., Munck, S., Ciotti, M.T., Zalfa, F., Mercanti, D., Molinari, M., Bagni, C., and Achsel, T. (2009). Dendritic LSm1/CBP80-mRNPs mark the early steps of transport commitment and translational control. J. Cell Biol. *184*, 423–435.

Doyle, M., and Kiebler, M.A. (2011). Mechanisms of dendritic mRNA transport and its role in synaptic tagging. EMBO J. *30*, 3540–3552.

Dubnau, J., Chiang, A.S., Grady, L., Barditch, J., Gossweiler, S., McNeil, J., Smith, P., Buldoc, F., Scott, R., Certa, U., et al. (2003). The staufen/pumilio pathway is involved in Drosophila long-term memory. Curr. Biol. *13*, 286–296.

Duchaîne, T.F., Hemraj, I., Furic, L., Deitinghoff, A., Kiebler, M.A., and DesGroseillers, L. (2002). Staufen2 isoforms localize to the somatodendritic domain of neurons and interact with different organelles. J. Cell Sci. *115*, 3285–3295.

Elvira, G., Wasiak, S., Blandford, V., Tong, X.K., Serrano, A., Fan, X., del Rayo Sánchez-Carbente, M., Servant, F., Bell, A.W., Boismenu, D., et al. (2006). Characterization of an RNA granule from developing brain. Mol. Cell. Proteomics *5*, 635–651.

Giorgi, C., Yeo, G.W., Stone, M.E., Katz, D.B., Burge, C., Turrigiano, G., and Moore, M.J. (2007). The EJC factor eIF4AIII modulates synaptic strength and neuronal protein expression. Cell *130*, 179–191.

Goetze, B., Tuebing, F., Xie, Y., Dorostkar, M.M., Thomas, S., Pehl, U., Boehm, S., Macchi, P., and Kiebler, M.A. (2006). The brain-specific double-stranded RNA-binding protein Staufen2 is required for dendritic spine morphogenesis. J. Cell Biol. *172*, 221–231.

Harlow, E., and Lane, D. (1988). Antibodies: A Laboratory Manual (Cold Spring Harbor: Cold Spring Harbor Laboratory Press).

Heraud-Farlow, J.E., Sharangdhar, T., Li, X., Pfeifer, P., Tauber, S., Orozco, D., Hörmann, A., Thomas, S., Bakosova, A., Farlow, A.R., et al. (2013). Staufen2 regulates neuronal target mRNAs. Cell Rep. *5*, this issue, 1511–1518.

Holt, C.E., and Bullock, S.L. (2009). Subcellular mRNA localization in animal cells and why it matters. Science *326*, 1212–1216.

Hüttelmaier, S., Zenklusen, D., Lederer, M., Dictenberg, J., Lorenz, M., Meng, X., Bassell, G.J., Condeelis, J., and Singer, R.H. (2005). Spatial regulation of beta-actin translation by Src-dependent phosphorylation of ZBP1. Nature *438*, 512–515.

Hwang, J., Sato, H., Tang, Y., Matsuda, D., and Maquat, L.E. (2010). UPF1 association with the cap-binding protein, CBP80, promotes nonsense-mediated mRNA decay at two distinct steps. Mol. Cell *39*, 396–409.

Jankowsky, E. (2011). RNA helicases at work: binding and rearranging. Trends Biochem. Sci. *36*, 19–29.

Jønson, L., Vikesaa, J., Krogh, A., Nielsen, L.K., Hansen, Tv., Borup, R., Johnsen, A.H., Christiansen, J., and Nielsen, F.C. (2007). Molecular composition of IMP1 ribonucleoprotein granules. Mol. Cell. Proteomics *6*, 798–811.

Kanai, Y., Dohmae, N., and Hirokawa, N. (2004). Kinesin transports RNA: isolation and characterization of an RNA-transporting granule. Neuron *43*, 513–525.

Kiebler, M.A., and Bassell, G.J. (2006). Neuronal RNA granules: movers and makers. Neuron *51*, 685–690.

Kiebler, M.A., López-García, J.C., and Leopold, P.L. (1999b). Purification and characterization of rat hippocampal CA3-dendritic spines associated with mossy fiber terminals. FEBS Lett. *445*, 80–86.

Kim, K.M., Cho, H., Choi, K., Kim, J., Kim, B.W., Ko, Y.G., Jang, S.K., and Kim, Y.K. (2009). A new MIF4G domain-containing protein, CTIF, directs nuclear cap-binding protein CBP80/20-dependent translation. Genes Dev. *23*, 2033–2045.

Köhrmann, M., Luo, M., Kaether, C., DesGroseillers, L., Dotti, C.G., and Kiebler, M.A. (1999). Microtubule-dependent recruitment of Staufen-green fluorescent protein into large RNA-containing granules and subsequent dendritic transport in living hippocampal neurons. Mol. Biol. Cell *10*, 2945–2953.

Konecna, A., Heraud, J.E., Schoderboeck, L., Raposo, A.A., and Kiebler, M.A. (2009). What are the roles of microRNAs at the mammalian synapse? Neurosci. Lett. *466*, 63–68.

Krichevsky, A.M., and Kosik, K.S. (2001). Neuronal RNA granules: a link between RNA localization and stimulation-dependent translation. Neuron *32*, 683–696.

Le Hir, H., and Séraphin, B. (2008). EJCs at the heart of translational control. Cell *133*, 213–216.

Macchi, P., Kroening, S., Palacios, I.M., Baldassa, S., Grunewald, B., Ambrosino, C., Goetze, B., Lupas, A., St Johnston, D., and Kiebler, M. (2003). Barentsz, a new component of the Staufen-containing ribonucleoprotein particles in mammalian cells, interacts with Staufen in an RNA-dependent manner. J. Neurosci. *23*, 5778–5788.

Maher-Laporte, M., Berthiaume, F., Moreau, M., Julien, L.A., Lapointe, G., Mourez, M., and DesGroseillers, L. (2010). Molecular composition of staufen2-containing ribonucleoproteins in embryonic rat brain. PLoS ONE *5*, e11350.

Mallardo, M., Deitinghoff, A., Müller, J., Goetze, B., Macchi, P., Peters, C., and Kiebler, M.A. (2003). Isolation and characterization of Staufen-containing ribonucleoprotein particles from rat brain. Proc. Natl. Acad. Sci. USA *100*, 2100–2105.

Martin, K.C., and Ephrussi, A. (2009). mRNA localization: gene expression in the spatial dimension. Cell *136*, 719–730.

Martin, S.G., Leclerc, V., Smith-Litière, K., and St Johnston, D. (2003). The identification of novel genes required for Drosophila anteroposterior axis formation in a germline clone screen using GFP-Staufen. Development *130*, 4201–4215.

Meister, G., Landthaler, M., Peters, L., Chen, P.Y., Urlaub, H., Lührmann, R., and Tuschl, T. (2005). Identification of novel argonaute-associated proteins. Curr. Biol. *15*, 2149–2155.

Mikl, M., Vendra, G., and Kiebler, M.A. (2011). Independent localization of MAP2, CaMKIIα and β-actin RNAs in low copy numbers. EMBO Rep. *12*, 1077–1084.

Palacios, I.M., Gatfield, D., St Johnston, D., and Izaurralde, E. (2004). An eIF4AIII-containing complex required for mRNA localization and nonsense-mediated mRNA decay. Nature *427*, 753–757.

Rappsilber, J., Ishihama, Y., and Mann, M. (2003). Stop and go extraction tips for matrix-assisted laser desorption/ionization, nanoelectrospray, and LC/MS sample pretreatment in proteomics. Anal. Chem. *75*, 663–670.

Shevchenko, A., Wilm, M., Vorm, O., and Mann, M. (1996). Mass spectrometric sequencing of proteins silver-stained polyacrylamide gels. Anal. Chem. *68*, 850–858.

Sisson, T.H., and Castor, C.W. (1990). An improved method for immobilizing IgG antibodies on protein A-agarose. J. Immunol. Methods *127*, 215–220.

St Johnston, D. (2005). Moving messages: the intracellular localization of mRNAs. Nat. Rev. Mol. Cell Biol. *6*, 363–375.

Sutton, M.A., and Schuman, E.M. (2006). Dendritic protein synthesis, synaptic plasticity, and memory. Cell *127*, 49–58.

Tang, S.J., Meulemans, D., Vazquez, L., Colaco, N., and Schuman, E. (2001). A role for a rat homolog of staufen in the transport of RNA to neuronal dendrites. Neuron *32*, 463–475.

Tiedge, H., and Brosius, J. (1996). Translational machinery in dendrites of hippocampal neurons in culture. J. Neurosci. *16*, 7171–7181.

Tübing, F., Vendra, G., Mikl, M., Macchi, P., Thomas, S., and Kiebler, M.A. (2010). Dendritically localized transcripts are sorted into distinct ribonucleoprotein particles that display fast directional motility along dendrites of hippocampal neurons. J. Neurosci. *30*, 4160–4170.

van Eeden, F.J., Palacios, I.M., Petronczki, M., Weston, M.J., and St Johnston, D. (2001). Barentsz is essential for the posterior localization of oskar mRNA and colocalizes with it to the posterior pole. J. Cell Biol. *154*, 511–523.

Vessey, J.P., Vaccani, A., Xie, Y., Dahm, R., Karra, D., Kiebler, M.A., and Macchi, P. (2006). Dendritic localization of the translational repressor Pumilio 2 and its contribution to dendritic stress granules. J. Neurosci. *26*, 6496–6508.

Vessey, J.P., Schoderboeck, L., Gingl, E., Luzi, E., Riefler, J., Di Leva, F., Karra, D., Thomas, S., Kiebler, M.A., and Macchi, P. (2010). Mammalian Pumilio 2 regulates dendrite morphogenesis and synaptic function. Proc. Natl. Acad. Sci. USA *107*, 3222–3227.

Vessey, J.P., Amadei, G., Burns, S.E., Kiebler, M.A., Kaplan, D.R., and Miller, F.D. (2012). An asymmetrically localized Staufen2-dependent RNA complex regulates maintenance of mammalian neural stem cells. Cell Stem Cell *11*, 517–528.

Villacé, P., Marión, R.M., and Ortín, J. (2004). The composition of Staufen-containing RNA granules from human cells indicates their role in the regulated transport and translation of messenger RNAs. Nucleic Acids Res. *32*, 2411–2420.

Wessel, D., and Flügge, U.I. (1984). A method for the quantitative recovery of protein in dilute solution in the presence of detergents and lipids. Anal. Biochem. *138*, 141–143.

Zeitelhofer, M., Karra, D., Macchi, P., Tolino, M., Thomas, S., Schwarz, M., Kiebler, M., and Dahm, R. (2008). Dynamic interaction between P-bodies and transport ribonucleoprotein particles in dendrites of mature hippocampal neurons. J. Neurosci. *28*, 7555–7562.

Zimyanin, V.L., Belaya, K., Pecreaux, J., Gilchrist, M.J., Clark, A., Davis, I., and St Johnston, D. (2008). In vivo imaging of oskar mRNA transport reveals the mechanism of posterior localization. Cell *134*, 843–853.